Proceedings of the 9th U.S. National and 10th Canadian Conference on Earthquake Engineering
Compte Rendu de la 9ième Conférence Nationale Américaine et
10ième Conférence Canadienne de Génie Parasismique
July 25-29, 2010, Toronto, Ontario, Canada • Paper No 1057

SYSTEMIC UNCERTAINTIES AND DECISION SUPPORT APPLICATIONS IN REGIONAL SEISMIC LOSS ANALYSES

J. S. Steelman[1] and J. F. Hajjar[2]

ABSTRACT

A number of tools and advancements have been developed over the course of the last decade for public use in regional seismic disaster planning. This paper addresses some of the considerations and approaches that influence state-of-the-art regional seismic loss assessments and risk management, with particular emphasis on approaches applied to areas having potentially high consequence but low probability seismic hazards in the United States. The various components of regional seismic loss assessment are synthesized within a GIS-based framework, including the aggregation and propagation of uncertainties inherent in the analysis. The threat posed by ground shaking and ground failure hazard effects is estimated and mapped onto high resolution point-wise building stock and bridge inventory assets. Inventory vulnerability is assigned based on structural classifications of construction materials, together with general system configurations and lateral resisting system types. Likelihood of damage to the built environment is then determined by the combination of the hazard and vulnerability for each building and bridge, and social and economic consequences are projected based on correlation with descriptions of physical damage levels, both in terms of expected values, and dispersions of the aggregate regional analysis output. Decision support algorithms are also discussed, which leverage the high resolution of the regional analysis output to focus mitigation planning and capital investment on particularly sensitive and influential assets within study regions.

Introduction

For more than a decade, many researchers and professional risk consultants worldwide have engaged in the development of seismic loss estimation methodologies, applied those methodologies to particular regions of interest, and published the findings in the literature. In the United States, multiple recent studies using HAZUS (FEMA 2006) have been documented for Charleston, SC (URS 2001), Northridge, CA (Reis et al. 2001), Seattle, WA (Ballantyne et al. 2005), and an eight state study of the New Madrid Seismic Zone (Elnashai et al. 2008).

[1]Graduate Research Assistant, Dept. of Civil Engineering, University of Illinois at Urbana-Champaign, Urbana, IL 61801
[2] Professor, Dept. of Civil Engineering, University of Illinois at Urbana-Champaign, Urbana, IL 61801

Numerous other commercial studies have been conducted worldwide, some of which have been performed by professional risk assessment firms using proprietary software. Among studies within academic research, notable published studies for losses on a regional scale include papers focusing heavily on western Turkey, as well as other Mediterranean areas such as Italy (e.g., Bal et al. 2008; Erdik et al. 2008; Teramo et al. 2008; Spence et al. 2008). Much of this work serves to form background and establish general guidelines of good practice when performing regional loss assessment.

This paper discusses a comprehensive procedure for regional loss assessment and decision support based on integration of several new algorithms within the open source, GIS-based environment of MAEViz (MAEViz 2008), using Shelby County, TN (including Memphis, TN) in the USA as a case study. One of the primary objectives for this case study was to investigate the influence of systemic uncertainties and propagate those uncertainties throughout the loss assessment. Also, in the early phases of this research, it was noted that strategies for decision-making and prioritizing mitigation efforts were not yet uniformly well established. Thus, a secondary objective was to explore the use of various decision support tools to leverage the data obtained from regional analyses in the interest of mitigating the effects of earthquakes for the population of the study region.

Risk Assessment

The core components of the regional seismic risk assessment in this work include: inventory collection, hazard definition, vulnerability assessment, and estimation of social and economic consequences. The general framework is similar to that applied in the other studies mentioned previously. Inventory information for Shelby County, TN was collected for buildings and bridges in the study region from several sources. Building-by-building data was acquired by extrapolating from tax record data through a neural network model, calibrated by surveys of sample buildings in the study region. Demographic information was extracted on a census track-basis, and disaggregated as required for algorithms that mesh with demographic data. Full details of sources and data processing are described in Steelman and Hajjar (2008). The building data is dominated by low-rise, light wood frame, single-family residential structures. Bridge data for the study region was obtained from the National Bridge Inventory and implemented as detailed in Steelman and Hajjar (2008).

To capture the true nature of a low-probability, high-consequence event, a seismic source was selected consistent with the historical seismology of the region. For this study, a moment magnitude of 7.9 was selected and located at Blytheville, AR, based on guidance provided by geotechnical experts within the Mid-America Earthquake Center. Attenuation equations developed by Fernandez and Rix (2006) were selected to account for the particular seismological characteristics of this region, which generally resulted in lower acceleration and higher displacement response of surface soils as a result of nonlinearity in the seismic soil response, compared to similar ground shaking estimates based on USGS attenuation functions and soil adjustment coefficients recommended by the U.S. National Earthquake Hazard Reduction Program (NEHRP).

The fragility formulations for the study region in this work were based on nonlinear time history analyses of various structure types. Several structure types were studied by various researchers constructing detailed models to capture the numerous complicated aspects inherent in nonlinear seismic response, as described in Steelman and Hajjar (2008). In the case of

structure types for which a fragility set had not been developed for the study region, or in the case of general nonstructural fragilities, a fragility set obtained from the modified parameterized fragility method (Jeong and Elnashai 2007, Steelman and Hajjar 2009) was employed, which incorporated the expected characteristics for the local ground motion in the study region (Fernandez 2007). Likewise, appropriate bridge fragilities, developed by MAE Center researchers, were also implemented to represent bridge construction typical of the Central and Eastern US as described in Steelman and Hajjar (2008). The required hazard input for each fragility set was determined by the researcher who originally performed each study. All fragilities took the form of a lognormal distribution.

The final component of the risk assessment included consideration of a range of individual metrics related to social and economic loss, with contributions from several MAE Center researchers, as described in Steelman and Hajjar (2008). In each case, probabilities of discrete damage states from the vulnerability assessment are combined with coefficients and demographic data as appropriate to provide estimates of losses. Sample aggregated results for the case study scenario are given in Table 1. Bridge functionality was also investigated, based on direct correlation from damage output of the vulnerability assessment. The transportation system is severely impacted by the earthquake, with only 2% of bridges fully operational immediately after the earthquake. Current predictions estimate, however, that many of the bridges that are damaged can be repaired within several days, contingent on availability of adequate materials and personnel.

Table 1. Risk Assessment Summary.

Buildings Repair / Replacement	$\$4.80 \times 10^9$
Bridges Repair / Replacement	$\$10.6 \times 10^6$
Hospitalizations	984
Fatalities	188
Business Interruption	$\$964 \times 10^6$
Business Inventory Damage	$\$83.8 \times 10^6$
Displaced Households	14,900
Displaced Persons	37,900
% Requiring Short Term Shelter	27.1
Loss of Property Tax Revenue	$\$42.4 \times 10^6$

Treatment of Systemic Uncertainties

As in many other regional seismic loss studies published in the literature, the primary direct impact is manifested in the repair and replacement component of building losses, as seen in Table 1. Consequently, the primary effort for quantification and treatment of uncertainties focused on that aspect of the risk assessment. Mean, $E[L_i]$, and variance, $VAR[L_i]$, of losses associated with repair and replacement costs for each inventory item, i, were determined according to the following equations.

$$E[L_i] = M_i \sum_{j=1}^{4} \alpha_j \mu_j \tag{1}$$

$$\mu_j = \sum_{k=1}^{4} P\left(DS = ds_k\right) * \mu_{DF_{k,j}} \tag{2}$$

$$VAR\left[L_i\right] = M_i^2 \sum_{j=1}^{4} \alpha_j^2 \sigma_j^2 \tag{3}$$

$$\sigma_j^2 = \sum_{k=1}^{4} \left[P\left(DS = ds_k\right) * \left(\sigma_{DF_{k,j}}^2 + \mu_{DF_{k,j}}^2\right)\right] - \mu_j^2 \tag{4}$$

where M_i is the replacement cost of a structure (exclusive of the value of its contents), α_j is a weighting factor to represent the influence of damage type j (e.g., structural, drift-sensitive nonstructural, acceleration-sensitive nonstructural, and contents) relative to the total value of M_i, and μ_j is the mean damage factor for damage type j from Eq. 2 (the term "damage factor" refers to a coefficient used to correlate physical damage to economic loss; the damage factor range varies with damage type and damage state, but always falls within the bounds of 0 to 1). $P(DS=ds_k)$ is the probability that the actual damage state, DS, is the k-th damage state (e.g., insignificant, moderate, heavy, complete), and $\mu_{DFk,j}$ is the mean damage factor for damage type j and damage state k. σ_j^2 is the variance of damage type j, and $\sigma_{DFk,i}^2$ is the variance of the damage factor for damage type j and damage state k.

Hazard Uncertainty Propagation

A method was determined to partially include the influence of hazard uncertainty in the estimates obtained from Eq 1 through Eq 4. The formula for determination of damage state probabilities of exceedence took the form

$$P\left(DS > ds_k \mid S_a\right) = \Phi\left(\frac{\ln\left(S_a\right) - \lambda_k}{\beta_k}\right) \tag{5}$$

where $P(DS > ds_k \mid S_a)$ is the probability that the damage to the inventory item under consideration will exceed the threshold of the k-th damage state, given a value of ground shaking acceleration, S_a. $\Phi(*)$ is the cumulative normal distribution evaluated at (*), S_a is the median ground shaking acceleration hazard appropriate for the fragility parameters, and λ_k and β_k are the lognormal median and dispersion parameters defining the threshold of k-th damage state. To partially account for hazard uncertainty, the β_k term was replaced with

$$\overline{\beta_k} = \sqrt{\beta_k^{\,2} + \beta_{Sa}^{\,2}} \tag{6}$$

in MAEViz, where β_{Sa} is the lognormal standard deviation of the ground shaking hazard. This approach is valid when the hazard and fragility functions be lognormally distributed. The shortcoming of this approach is that it is limited to the consideration of a single damage type, although the algorithms employed in this study considered structural, drift-sensitive nonstructural, acceleration-sensitive nonstructural, and contents damage types and losses

separately. Consequently, when combining damage estimation from various damage types, the shared dependence on hazard is not maintained.

Correlation of Hazard Uncertainty Between Damage Types

To investigate the comprehensive influence of shared hazard between damage types, numerical integrations across a range of ground acceleration values were performed for several sets of input parameters, varying hazard median and dispersion inputs according to attenuation functions and epicenter distance, and fragility parameters according to structure types. All fragilities were taken from a dataset developed by applying the parameterized fragility method (Jeong and Elnashai 2007, Steelman and Hajjar 2009), and, to limit the scope of this study on correlation of hazard uncertainty to different damage types, considering only low-rise, pre-code, single-family residence structures, which represent the clear majority of structures within the study region.

For each combination of parameters, total damage factor distributions, equivalent to Eq. 1 normalized by the sum of M_i and the estimated value of contents, were evaluated for a range of ground acceleration values. The output at each individual ground acceleration was then weighted according to the probability density function of the ground acceleration distribution, and numerically integrated to arrive at the overall probability density function of the total damage factor. An example result of this process is shown in Figure 1(a), which plots total direct damage factors, i.e., damage ratios, versus probability density. The assumed structure type was a light wood frame, and the lognormal ground acceleration median and dispersion values were 0.43g and 0.674. The means of each plotted distribution are similar, with the numerical integration and fitted beta distribution approximation differing from the MAEViz result (including the modification shown in Eq. 6) by -0.25%. The variance, however, increased from 0.019 to 0.035, an increase of 85%, when considering the correlation of hazard between damage types. These results reflect the fact that the mean value of the loss estimate is accurately captured solely by the adjustment in Eq. 6. However, the uncertainty of the loss estimate was underestimated because hazard correlation between damage types was not included in Eq 3. Thus, the consideration of hazard correlation between damage types is necessary to accurately represent the dispersion of the total loss estimate for each building in the inventory.

For the scenarios and study region considered, the inclusion of hazard uncertainty was found to generally increase the mean expected loss. The degree to which this occurred depended on the fragility parameters, α_j coefficients, and damage factors for various damage types and states, in addition to the hazard median and dispersion values. When using attenuation functions developed within the MAE Center and a source event located at Blytheville, AR, with a moment magnitude of 7.9, the increase of the mean expected loss ranged from 9% to 21% when using single-family residence α_j coefficients and pre-code, low-rise fragility parameters. When USGS attenuation functions and NEHRP soil factors for Site Class D were substituted, both the hazard median and dispersion increased for the same source event. The result of this change was a wider dispersion of influence, with modifications of -2% to 54%, depending on the specific combination of hazard and fragility parameters.

To illustrate the effect of hazard uncertainty on loss estimation dispersion, 90% confidence bounds of damage factor distributions were evaluated for a baseline case neglecting hazard uncertainty, then with the MAEViz algorithm, and finally with the additional consideration of hazard correlation across damage types. Figure 1(b) is provided as a key for

Figures 2(a) and 2(b). In Figure 1(b), damage ratio distributions are plotted for each case, with superimposed bars indicating ranges of 90% confidence on the left side of the figure, and stacked bars on the right side of the figure. Figures 2(a) and 2(b) show 90% confidence ranges for common structure types, based on MAE Center and USGS/NEHRP hazard estimates, respectively, using a source moment magnitude of 7.9 at about 60 km epicenter distance. Structure types are given codes (Steelman and Hajjar 2008), such as C for concrete, S for steel, W for wood, and so on. The effect of damage type correlation varies with structure type, based on the fragility parameters used to define each structure. The estimated hazard uncertainty increases significantly when using the USGS/NEHRP attenuation functions, and this difference has a strong effect on increasing the range of 90% confidence for the damage ratio estimate.

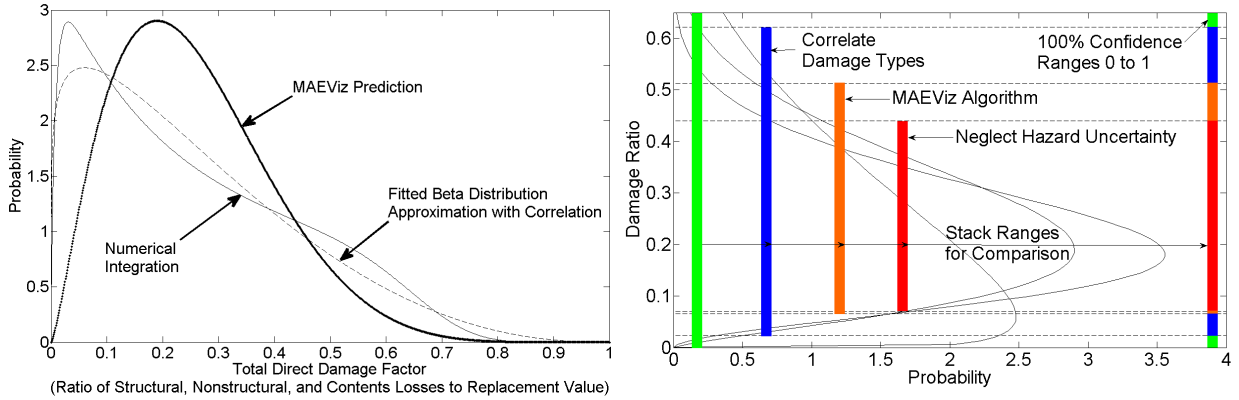

(a) (b)

Figure 1. Graphical representations of (a) alternative damage factor probability density distributions, and (b) stacked 90% confidence ranges of damage ratio distributions.

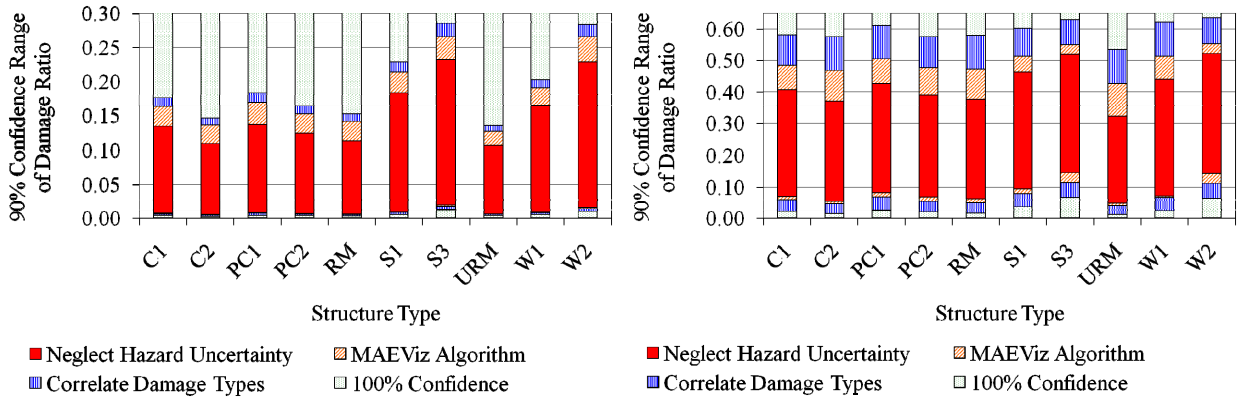

(a) (b)

Figure 2. 90% total loss ratio confidence ranges for structure types using (a) MAE Center hazard, and (b) USGS/NEHRP hazard.

Generalized Method for Damage Type Hazard Correlation

The prospect of performing the numerical integration across a range of ground acceleration values for all structures in a study region is computationally demanding for large study regions. To approximate the effect of correlation between damage types, a relation may be

developed to address large groups of structures, as shown in Figure 3. The data used to develop the surface plot shown in Figure 3 are appropriate for light wood frame single-family residences, using the fragility parameters associated with the threshold between moderate and heavy damage, and scaling hazard parameters from 0.1 to 2 times the fragility parameters in steps of 0.1. The data may be fit to an expression, as

$$\frac{VAR_{CORR}}{VAR_{UNCORR}} = \gamma_1 \left(\frac{e^{\lambda_{hazard}}}{e^{\lambda_{fragility}}} \right) + \gamma_2 \left(\frac{\beta_{hazard}}{\beta_{fragility}} \right) + \gamma_3 \tag{7}$$

where the γ_i terms are regression fit parameters, and λ and β are lognormal median and dispersion of hazard or fragility, as indicated in the subscripts.

Recalling the values provided in the previous section, with γ_1, γ_2, and γ_3 determined by fitting to be 0.1349, 0.6013, and 0.7358, respectively, and also with the ratios of hazard to fragility median and dispersion equal to (0.43g / 0.488g = 0.881) and (0.674 / 0.448 = 1.50), respectively, Eq 7 evaluates to 1.76, or a 76% increase, when considering the correlation of hazard between damage types. This is compared to the value of 85% obtained by numerical integration above. The agreement can be improved by truncating the component influenced by γ_1 to remove the bias included in the fit from small earthquakes. When calculations were performed for other structure types and occupancy class combinations, the maximum and minimum ratios of γ_2 / γ_1 were 6.34 and 1.59, maximum and minimum values of γ_2 were 0.684 and 0.277, and maximum and minimum values of γ_1 were 0.213 and 0.051. These fit parameters reflect the fact that the correlation of damage types depends on both the median and dispersion of hazard values, but there is much greater sensitivity to the hazard estimate dispersion.

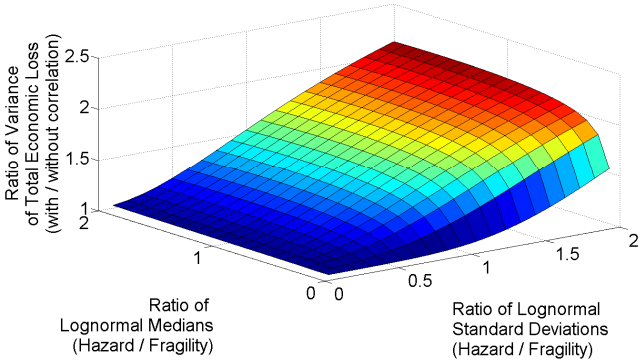

Figure 3. Surface plot of ratio of total loss with and without damage type hazard correlation.

Decision Support

For the case study region, two methods of mitigation planning and prioritization (i.e., decision support) were employed: Comparative Equivalent Cost Analysis (ECA) and Multi-Attribute Utility Analysis (MAUA) (Steelman and Hajjar 2008).

Comparative Equivalent Cost Analysis

For ECA, the primary calibration involves assigning dollar values to certain key

commodities that do not inherently have a dollar value associated with them, such as a casualty. For this study, estimates were developed based on forensic economic literature, as described in Steelman and Hajjar (2008), so that a death was estimated to be worth approximately $8.5 million, and an injury was estimated to be worth $1 million. Additional required data to perform the ECA include vulnerability data for retrofit options and some method of estimating costs to install retrofits. The approach used for these scenarios was to develop additional fragility sets using the parameterized fragility method, as described previously, including implementing parameters (e.g., strength ratio, period) tabulated for higher (i.e., improved) "code levels" in the HAZUS documentation. Costs were estimated for these retrofits based on literature as described in Steelman and Hajjar (2008). The optimum retrofit assignments were calculated for each building in the study region, based on maximizing the cost-benefit ratio and ensuring that only ratios greater than one were acceptable.

The cost to install all optimum retrofits is $602 million. However, when reviewing the results at the building level, a subset of buildings is found to provide exceptionally high benefit in return for the required investment. A group of eight hospitals provide benefit-cost ratios in excess of 40. The selected hospital locations are indicated in Figure 4 as white circles overlaying a map of hospitalizations by tract. The total cost to retrofit this subset is estimated at $10.5 million, but the total projected benefit is $555.6 million. This subset of buildings also happens to share the same structure type: steel frame. Although not explicitly considered algorithmically, the selected subset may potentially permit the use of similar retrofit designs and details for multiple buildings.

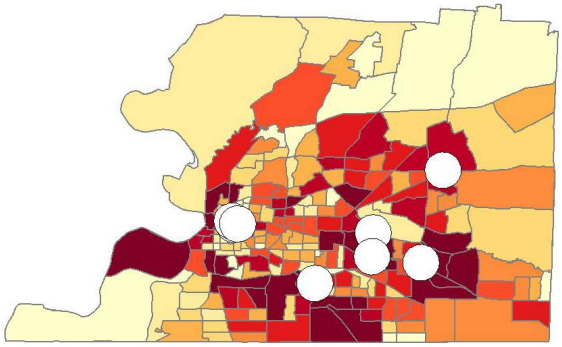

Figure 4. Selected retrofits according to ECA.

Multi-Attribute Utility Analysis

The MAUA, in turn, seeks to quantify performance parameters of the region in a relative "utility" sense. In this context, utility may be viewed as an indicator of satisfaction. The maximum value is 1, and this is assumed to be the value for the study region prior to the earthquake. As repair costs increase and casualties mount, the utility drops. The utility function can be any non-increasing function desired by a decision-maker. For this case study, two functions were implemented to reflect two risk attitudes: a cubic function to represent a risk-averse attitude, and an exponential to represent a risk-seeking attitude. The limit parameters for the analyses were determined by scaling and calibrating from published losses for the 1994 Northridge earthquake. Limits of 621 persons killed, 3249 persons injured, and a total economic loss of $4.8 billion were used to establish thresholds of zero utility.

Optimum retrofits were established for these cases by computing a change in utility for

the region resulting from installation of a retrofit, and then normalizing that change in utility for the study region by the cost of the retrofit. The decision-making influences were also varied as part of the study by considering four cases. To calculate utility for a region, the individual utility values are weighted and summed, so the relative influences of various concerns can be incorporated by scaling weighting factors. The four cases considered, with values established in this work, were: (1) 0.25 weight for economic loss, injuries, fatalities, and loss of essential facility functionality, (2) 0.85 weight on economic loss, (3) 0.45 weight on each of injuries and fatalities, and (4) 0.85 weight on essential facility functionality. Figures 5(a) and 5(b) show optimum retrofits based on utility gradient for cases 2 and 3, respectively.

The results in Figure 5(a), in particular, are fairly similar to the ECA result. As shown in Figures 5(a) and 5(b), the weight attributed to the value of life by a decision-maker has a pronounced effect on the result of the analysis. The calculations that lead up to the risk assessment, combined with the calculations for the various retrofit options for each structure are computationally intensive, but the final output, in this case, provides direct guidance for the most attractive retrofit options for each structure in the region.

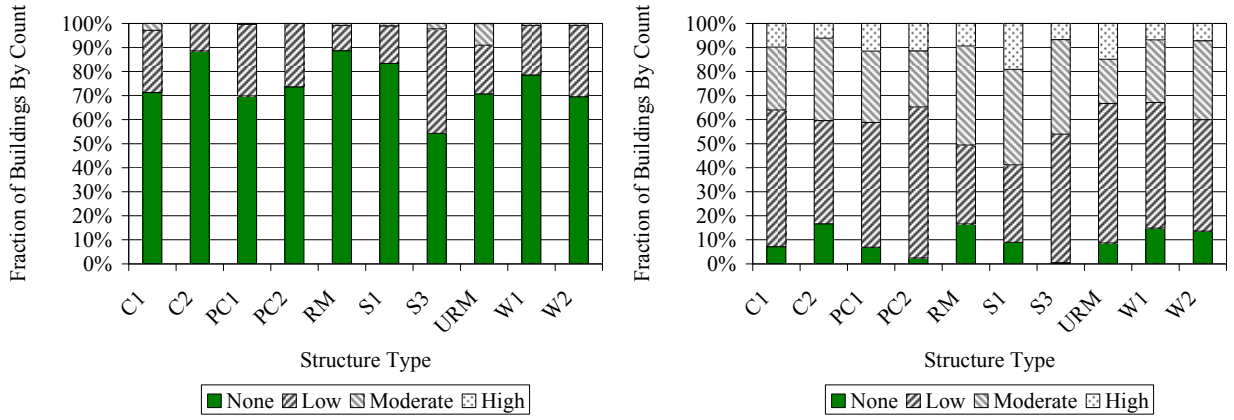

Figure 5. Optimum retrofit code levels for MAUA to minimize (a) direct economic loss and (b) casualties.

Conclusions

This paper summarized findings from an investigation into the reliability of expected values for seismic risk assessments. It is shown that shifts in direct economic loss estimations resulting from incorporation of ground shaking uncertainty can be achieved through a simple algorithmic adjustment to the typical equation used to estimate probabilities of damage states. Furthermore, to fully capture the influence of ground shaking uncertainty on the loss estimation uncertainty, numerical integration is necessary to merge uncertainty across components of direct damage (structural, nonstructural, etc.). A relation is postulated to correlate ratios of hazard and fragility median and dispersion parameters with the ratio of coefficient of variation with and without consideration of damage type correlation.

Two algorithms suited to evaluating competing retrofit options based on direct effects were presented. The primary consideration for both algorithms is to select suitable decision weights. This presents decision-makers with a conundrum when requiring the assignment of definitive values and influence to considerations of human life, pain, and suffering. However,

reasonable values can be estimated from forensic literature and incorporated into regional seismic risk assessments to arrive at justifiable retrofit strategies. Furthermore, the utilization of point-wise inventory allows the prioritization, building-by-building, as a part of the retrofit plan.

Acknowledgments

This research was supported by the Mid-America Earthquake Center, headquartered at the University of Illinois at Urbana-Champaign, under NSF Grant No. EEC-97010785, and by the University of Illinois at Urbana-Champaign. The authors would like to thank the researchers throughout the MAE Center who have provided information for this research. Any opinions, findings, and conclusions or recommendations expressed in this material are those of the authors and do not necessarily reflect the views of the National Science Foundation or other sponsors.

References

Bal, I.E., H. Crowley, and R. Pinho, 2008. Development of a Displacement-Based Earthquake Loss Assessment Method for Turkish Buildings, 14WCEE, Beijing, China, October 12-17, 2008, Intl. Assoc. of Earthq. Engrg., Beijing, China.

Ballantyne, D., S. Bartoletti, S. Chang, B. Graff, G. MacRae, J. Meszaros, I. Pearce, M. Pierepiekarz, J. Preuss, M. Stewart, D. Swanson, and C. Weaver, 2005. *Scenario for a Magnitude 6.7 Earthquake on the Seattle Fault*, Earthquake Engineering Research Institute, Oakland, California.

Elnashai, A.S., L. J. Cleveland, T. Jefferson, and J. Harrald, 2008. *Impact of Earthquakes on the Central USA*, Mid-America Earthquake Center, U. of IL, Urbana, IL.

Erdik, M., Z. Cagnan, C. Zulfikar, K. Sesetyan, M.B. Demircioglu, E. Durukal, and C. Kariptas, 2008. Development of Rapid Earthquake Loss Assessment Methodologies for Euro-Med Region, 14WCEE, Beijing, China, October 12-17, 2008, Intl. Assoc. of Earthq. Engrg., Beijing, China.

Federal Emergency Management Agency (FEMA), 2006. *HAZUS-MH MR2 Users and Technical Manual*, Federal Emergency Management Agency, Washington, D.C.

Fernandez, J.A., 2007. Numerical Simulation of Earthquake Ground Motions in the Upper Mississippi Embayment, *Ph.D. Thesis*, School of Civil and Environmental Engineering, Georgia Institute of Technology, Atlanta, GA.

Fernandez, J.A. and G.J. Rix, 2006. Soil Attenuation Relationships and Seismic Hazard Analyses in the Upper Mississippi Embayment. Proceedings of the 8th U.S. National Conference on Earthquake Engineering, San Francisco, California, April 18-22, 2006, Earthquake Engineering Research Institute, Oakland, CA.

Jeong, S.H., and A.S. Elnashai, 2007. Probabilistic Fragility Analysis Parameterized by Fundamental Response Quantities, *Engineering Structures* 29, 1238-1251.

MAEviz, 2008. MAEviz Software, Mid-America Earthquake Center, U. of IL, Urbana, IL.

Pinho, R., H. Crowley, and J. Bommer, 2008. Open-Source Software and Treatment of Epistemic Uncertainties in Earthquake Loss Modelling, 14WCEE, Beijing, China, October 12-17, 2008, Intl. Assoc. of Earthq. Engrg., Beijing, China.

Reis, E., C. Comartin, S. King, and S. Chang, 2001. *HAZUS99-SR1 Validation Study*, Federal Emergency Management Agency, Washington, D.C.

Spence, R., E. So, G. Cultrera, A. Ansal, K. Pitilakis, A.C. Costa, G. Tonuk, S. Argyroudis, K. Kakderi, and M.L. Sousa, 2008. Earthquake Loss Estimation and Mitigation in Europe: A Review and Comparison of Alternative Approaches, 14WCEE, Beijing, China, October 12-17, 2008, Intl. Assoc. of Earthq. Engrg., Beijing, China.

Steelman, J.S., and J.F. Hajjar, 2008. Capstone Scenario Applications of Consequence-Based Risk Management for the Memphis Testbed, Mid-America Earthquake Center, U. of IL Urbana, IL.

Steelman, J.S., and J.F. Hajjar, 2009. Influence of inelastic seismic response modeling on regional loss estimation, *Engineering Structures,* in press.

Teramo, M., H. Crowley, M. Lopez, R. Pinho, G. Cultrera, A. Cirella, M. Cocco, M. Mai, and A. Teramo, 2008. A Damage Scenario for the City of Messina, Italy, Using Displacement-Based Loss Assessment, 14WCEE, Beijing, China, October 12-17, 2008, Intl. Assoc. of Earthq. Engrg., Beijing, China.

URS Corporation 2001. Comprehensive Seismic Risk and Vulnerability Study for the State of South Carolina, Internal Rep., South Carolina Emergency Preparedness Division, West Columbia, SC.